

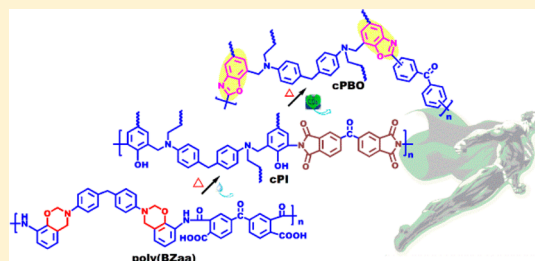
# An Ultrahigh Performance Cross-Linked Polybenzoxazole via Thermal Conversion from Poly(benzoxazine amic acid) Based on Smart *o*-Benzoxazine Chemistry

Kan Zhang,<sup>†,‡</sup> Jia Liu,<sup>‡</sup> and Hatsuo Ishida<sup>\*,‡</sup>

<sup>†</sup>School of Materials Science and Engineering, East China University of Science and Technology, Shanghai 200237, China

<sup>‡</sup>Department of Macromolecular Science and Engineering, Case Western Reserve University, Cleveland, Ohio 44106, United States

**ABSTRACT:** A main-chain-type polybenzoxazine with amic acid and benzoxazine groups as repeating units, generally termed as poly(benzoxazine amic acid) (poly(BZaa)), has been synthesized. Different from traditional main-chain polybenzoxazines, poly(BZaa) can undergo polymerization and imidization reactions to form cross-linked polyimide (cPI) after certain thermal treatment. cPI can further undergo a typical cyclization to give cross-linked polybenzoxazole (cPBO) after an additional thermal treatment. A model reaction is designed based on the reaction of 3-phenyl-2,4-dihydro-2*H*-benzo[*e*][1,3]oxazin-9-amine with a phthalic anhydride. Fourier transform infrared (FTIR) and proton nuclear magnetic resonance (<sup>1</sup>H NMR) spectroscopies are used to confirm the structure of model compound. The ring-opening polymerization behavior of benzoxazine monomers and main-chain polybenzoxazine is studied by differential scanning calorimetry (DSC). Thermal properties of the cross-linked polymers are also studied by dynamic mechanical analysis (DMA) and thermogravimetric analysis (TGA).



## INTRODUCTION

Aromatic polymer films have attracted much attention in the microelectronic and aerospace applications due to their excellent thermal, electronic, and mechanical properties.<sup>1</sup> Among these polymers, polybenzoxazoles (PBOs) have superior thermal stabilities compared to any other rigid polymers, such as polyimides and polybenzimidzoles.<sup>1,2</sup> However, the very high rigidity of PBOs also leads to difficulties in synthesis and fabrication. One possible approach to prepare PBO film is the use of a strong acid, such as poly(phosphoric acid) (PPA), which can dissolve PBOs.<sup>3</sup> However, the use of such strong acid is environmentally unfriendly and unfavorable in a view of manufacturing. The residual acid can also lead to aging problems as well under humid and warm application conditions. Thus, the fabrication of PBOs without the use of strong acid as solvent is strongly desired. Another way is to develop a PBO precursor that is soluble in organic solvent.<sup>4,5</sup>

Polybenzoxazine (PBz) has attracted much attention due to its excellent mechanical and thermal properties with good handling capability for material processing and composite manufacturing.<sup>6–13</sup> Benzoxazines can be polymerized through the cationic ring-opening of oxazine ring with or without an added initiator and/or catalyst. Besides, their extraordinarily rich molecular design flexibility allows designing various molecular structures with desired properties. Moreover, they release no reaction byproduct during the ring-opening polymerization reactions. No strong acid or alkaline catalysts are required for the synthesis of monomers. However, some acids, such as carboxylic acids and phenols, will accelerate the

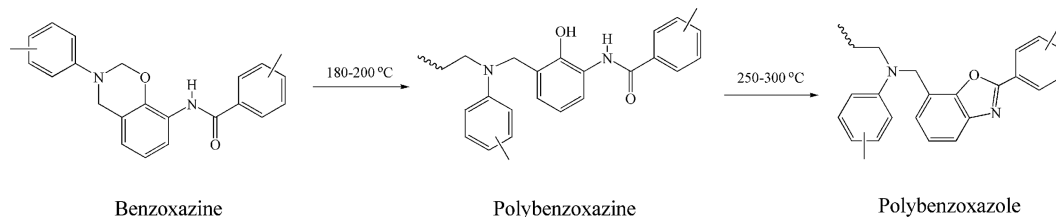
rate of polymerization. Furthermore, no volatiles are released, and nearly zero shrinkage is achieved upon polymerization.

Recently, we developed a new class of cross-linked PBOs via thermal conversion from *ortho*-amide functional benzoxazines as shown in Scheme 1.<sup>14</sup> The cross-linked PBOs show further advantages including excellent flexibility in the molecular design, easy processability, and cost effectiveness. Among this novel class of cross-linkable PBOs, the polybenzoxazole based on main-chain type shows the best balance of thermal stability, mechanical properties, and flame resistance. However, the synthesis of main-chain-type benzoxazine polymers through Mannich base polycondensation results in few shortcomings, such as poor solubility of the products due to molecular rigidity, leading to a low molecular weight and broad polydispersity. In our previous work, we prepared benzoxazine with primary amine using protection and deprotection methods<sup>15</sup> and then used the primary amine-containing benzoxazines to prepare a main-chain-type poly(benzoxazine amide).<sup>16</sup> In addition, Lin et al. also prepared primary-amine-containing benzoxazines by the steric hindrance control method. On the basis of the primary amine-containing benzoxazines, they prepared poly(benzoxazine imide) thermosets. The experimental results show that incorporating benzoxazine into polyimides increased the *T<sub>g</sub>*, tensile modules, flame retardancy, dimensional stability, and contact angle without losing too much in thermal stability.<sup>17</sup>

Received: November 13, 2014

Revised: December 4, 2014

Published: December 11, 2014

Scheme 1. Synthesis of Polybenzoxazole via Thermal Conversion from *ortho*-Amide Functional Benzoxazine

From all these findings, we were encouraged to find a smart approach to prepare the ultrahigh performance cross-linked PBOs based on the main-chain-type benzoxazine. We define the words “ultrahigh performance polymers” in thermal properties as those polymers that possess 5 wt % weight reduction temperature,  $T_{ds}$ , above 500 °C in this paper. In this article, we prepared *ortho*-amine-functional benzoxazines by protection of the amino group in *o*-aminophenol using tetrachlorophthalimide (TCP), carried out the benzoxazine synthesis, and then deprotected the TCP-protected benzoxazine using hydrazine hydrate. The yield of the *ortho*-amine-functional benzoxazines is much higher compared with our previous work of *para*-amine-functional benzoxazines by the TCP-protected method. Besides, we also prepared a main-chain-type poly(benzoxazine amic acid) (Poly(BZaa)) based on the *ortho*-amine-bifunctional benzoxazine with 3,3',4,4'-benzophenonetetracarboxylic dianhydride (BTDA). Since we already know that the *ortho*-amide-functional benzoxazines can be polymerized and further thermal treatment to give polybenzoxazoles based on our previous work,<sup>14</sup> and Mathias and others reported the possible thermal conversion of *ortho*-hydroxy-polyimides into polybenzoxazoles with releasing carbon dioxide at temperature around 400 °C,<sup>18–21</sup> we reasonably predict this main-chain-type poly(BZaa) should undergo an very interesting thermal behavior. The detailed synthetic strategy and the thermal behavior of benzoxazine amic acid will be discussed in this article.

## EXPERIMENTAL SECTION

**Materials.** *o*-Aminophenol (>98%), tetrachlorophthalic anhydride (99%), paraformaldehyde (99%), 3,3',4,4'-benzophenonetetracarboxylic dianhydride (BTDA), and phthalic anhydride were used as received from Sigma-Aldrich. 4,4'-Diaminodiphenylmethane (DDM, 98%) and aniline were purchased from Aldrich. Chloroform, dimethylacetamide, hexane, xylenes, methanol, and sodium sulfate were purchased from Fisher Scientific and used as received.

**Characterization.** Proton nuclear magnetic resonance (<sup>1</sup>H NMR) spectra were recorded on a Varian Oxford AS300 (300 MHz) using chloroform (CDCl<sub>3</sub>) and dimethyl sulfoxide (DMSO-*d*<sub>6</sub>) as solvent. The average number of transients for <sup>1</sup>H MNR measurement was 64. When quantitative information was desired, the contact time of 10 s was utilized. Fourier transform infrared (FTIR) spectra were measured by a Bomem Michelson MB100 FTIR spectrometer, which was connected with a dry air purge unit and a deuterated triglycine sulfate (DTGS) detector. Sixty-four scans were coadded to obtain a spectrum at a resolution of 4 cm<sup>-1</sup>. All powdered samples were finely ground with KBr powder and pressed into a disk, and the spectrum was taken as the transmission mode. Differential scanning calorimeter (DSC) measurements were conducted with a TA Instruments DSC Model 2920 using nitrogen as a purge gas (60 mL/min) at a heating rate of 10 °C/min. All samples were sealed using hermetic aluminum pans and covered with lids. Dynamic mechanical analysis (DMA) was performed on a TA Instruments Model Q800 DMA applying controlled strain tension mode with amplitude of 10 μm and a ramp rate of 3 °C/min. Strain sweep was first performed to determine the

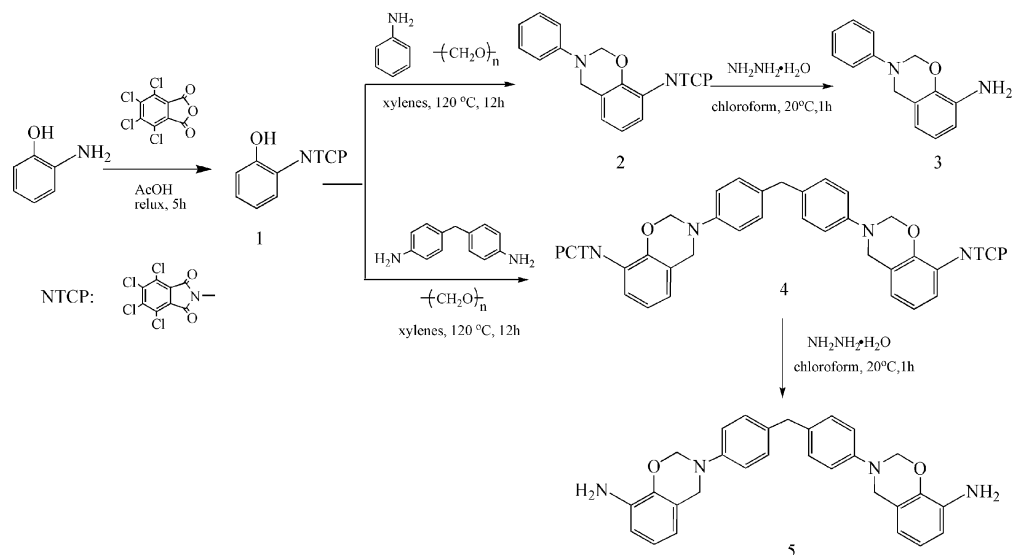
linear viscoelastic limit. Thermogravimetric analysis (TGA) was performed by a TA Instruments Q500 TGA using nitrogen as a purge gas (40 mL/min) at a heating ramp rate of 10 °C/min. Micro-Raman scattering measurements were done by a Horiba Jobin Yvon LabRam HR800 spectrometer connected with a charge coupled detector and two grating systems (600 and 1800 lines/min) at room temperature. The optical power of the He–Ne laser used was 17 W at 632.8 nm. The system was calibrated using the silicon line at 520 cm<sup>-1</sup>.

**Preparation of 4,5,6,7-Tetrachloro-2-(2-hydroxyphenyl)-isoindoline-1,3-dione (1).** Tetrachlorophthalic anhydride (13.75 g, 0.048 mol), *o*-aminophenol (5.77 g, 0.0523 mol), and 100 mL of acetic acid were mixed in a 250 mL round flask equipped with a reflux condenser. The mixture was stirred and refluxed at 120 °C for 6 h. Then the reaction mixture was cooled to room temperature. The precipitate was filtered and washed with 300 mL of methanol. Removal of solvent by evaporation afforded a yellow crystal (yield ca. 89%). <sup>1</sup>H NMR (300 MHz, DMSO-*d*<sub>6</sub>), ppm: δ = 6.87–7.36 (4H, Ar), 9.93 (OH). IR spectra (KBr, cm<sup>-1</sup>) = 3414 (O–H stretching), 1782, 1717 (imide I), 1304 (imide II, C–N stretching), 741 (C=O bending).

**Preparation of 4,5,6,7-Tetrachloro-2-(3-phenyl-3,4-dihydro-2H-benzo[e][1,3]oxazin-8-yl)isoindoline-1,3-dione (2).** 80 mL of xylenes, aniline (3.72 g, 0.04 mol), **1** (15.18 g, 0.04 mol), and paraformaldehyde (2.41 g, 0.08 mol) were mixed in a 250 mL round flask equipped with a reflux condenser. The mixture was heated and refluxed at 120 °C for 12 h. Then the reaction solution was cooled to room temperature and precipitated into 150 mL of methanol. A yellow powder product was obtained by evaporation the solvent under vacuum (yield ca. 95%). <sup>1</sup>H NMR (300 MHz, DMSO-*d*<sub>6</sub>), ppm: δ = 4.73 (s, Ar–CH<sub>2</sub>–N, oxazine), 5.44 (s, O–CH<sub>2</sub>–N, oxazine), 6.82–7.31 (8H, Ar). IR spectra (KBr, cm<sup>-1</sup>): 1786, 1730 (imide I), 1484 (stretching of trisubstituted benzene ring), 1390 (imide II), 1220 (C–O–C asymmetric stretching), 1161 (C–N–C asymmetric stretching), 932 (out-of-plane C–H).

**Preparation of 3-Phenyl-3,4-dihydro-2H-benzo[e][1,3]-oxazin-8-amine (3) by Deprotection of 2.** TCP-protected monofunctional benzoxazine (**2**) (4.91 g, 0.01 mol) and 60 mL of chloroform were mixed in a 250 mL round flask. The mixture was stirred in an ice bath for 15 min. Then the addition of hydrazine monohydrate (1.5 g, 0.03 mol) was added to the suspension. The mixture was stirred for 1 h at room temperature, followed by filtration of the solid residues. The filtrate was washed by 0.5 N aqueous NaOH solution for one time and then washed with water for 3 times. After that, the solution was dried over sodium sulfate anhydrous. The solvent was removed by evaporation using a rotary evaporator under reduced pressure. Finally, a brown color semisolid material was obtained (yield: 82%). <sup>1</sup>H NMR (300 MHz, CDCl<sub>3</sub>), ppm: δ = 3.72 (s, NH<sub>2</sub>), 4.62 (s, Ar–CH<sub>2</sub>–N, oxazine), 5.42 (s, O–CH<sub>2</sub>–N, oxazine), 6.46–7.31 (8H, Ar). IR spectra (KBr, cm<sup>-1</sup>): 3356 (N–H stretching), 1497 (stretching of trisubstituted benzene ring), 1222 (C–O–C asymmetric stretching), 1149 (C–N–C asymmetric stretching), 930 (out-of-plane C–H).

**Preparation of 2,2'-(3,3'-(4,4'-Methylenebis(2,1-phenylene))-bis(3,4-dihydro-2H-benzo[e][1,3]oxazin-8,3-diyl))bis(4,5,6,7-tetrachloroisoindoline-1,3-dione) (4).** 50 mL of xylenes, DDM (1.05 g, 5.3 mmol), **1** (4 g, 0.011 mol), and paraformaldehyde (0.75 g, 0.025 mol) were mixed in a 250 mL round flask equipped with a reflux condenser. The mixture was stirred and refluxed at 120 °C for 12 h. Then the reaction solution was cooled to room temperature and precipitated into 250 mL of methanol. A yellow powder product was

Scheme 2. Preparation of Amine-Functional Benzoxazine Monomers Using TCP-Protected *o*-Aminophenol

obtained by evaporation the solvent under vacuum (yield ca. 86%).  $^1\text{H}$  NMR (300 MHz,  $\text{DMSO}-d_6$ ), ppm:  $\delta$  = 3.71 (s,  $\text{CH}_2$ ), 4.65 (s,  $\text{CH}_2$ , oxazine), 5.37 (s,  $\text{CH}_2$ , oxazine), 6.39–7.28 (14H, Ar). IR spectra (KBr),  $\text{cm}^{-1}$ : 1786, 1730 (imide I), 1513 (stretching of trisubstituted benzene ring), 1390 (imide II), 1218 (C–O–C asymmetric stretching), 1129 (C–N–C asymmetric stretching), 925 (out-of-plane C–H).

**Preparation of 3,3'-(4,4'-Methylenebis(2,1-phenylene))bis-(3,4-dihydro-2H-benzo[e][1,3]oxazin-8-amine) (5) by Deprotection of 4.** Into a 50 mL round flask was added TCP-protected difunctional benzoxazine (**4**) (1 g, 2.152 mmol) and 15 mL of chloroform. The mixture was stirred in an ice bath for 15 min. Then the addition of hydrazine monohydrate (0.645 g, 12.915 mmol) was added to the suspension. The reaction solution was stirred for 1 h at room temperature, followed by filtration of the solid residues. The filtrate was washed by 0.5 N aqueous NaOH solution for one time and then washed with water for 3 times. After that, the solution was dried over sodium sulfate anhydrous. The solvent was removed by evaporation using a rotary evaporator under reduced pressure. Finally, a pinkish powder was obtained (yield 80%).  $^1\text{H}$  NMR (300 MHz,  $\text{CDCl}_3$ ), ppm:  $\delta$  = 3.69 (s,  $\text{NH}_2$ ), 3.81 (s,  $\text{CH}_2$ ), 4.56 (s, Ar– $\text{CH}_2$ –N, oxazine), 5.36 (s, O– $\text{CH}_2$ –N, oxazine), 6.37–7.26 (14H, Ar). FTIR spectra (KBr),  $\text{cm}^{-1}$ : 3307 (N–H stretching), 1502 (stretching of trisubstituted benzene ring), 1230 (C–O–C asymmetric stretching), 1153 (C–N–C asymmetric stretching), 928 (out-of-plane C–H).

**Preparation of Benzoxazine Amic Acid Model Compound (6).** 20 mL of DMAc, 3 (1 g, 4.4 mmol), and phthalic anhydride (0.66 g, 4.4 mmol) were mixed into a 50 mL round flask. The reaction solution was stirred for 4 h in an ice bath. Then the mixture was poured into water. The precipitate was filtered and dried in a vacuum oven at 50 °C to give an orange crystal (yield ca. 83%).  $^1\text{H}$  NMR (300 MHz,  $\text{CDCl}_3$ ), ppm:  $\delta$  = 4.64 (s, Ar– $\text{CH}_2$ –N, oxazine), 5.40 (s, O– $\text{CH}_2$ –N, oxazine), 6.68–8.30 (12H, Ar), 10.30 (s, NH). IR spectra (KBr),  $\text{cm}^{-1}$ : 3412 (carboxylic acid), 1721 (carbonyl absorption), 1681 (amide I), 1497 (stretching of trisubstituted benzene ring), 1257 (C–O–C asymmetric stretching), 1144 (C–N–C asymmetric stretching), 925 (out-of-plane C–H).

**Preparation of Poly(benzoxazine amic acid) (Poly(BZaa)), Cross-Linked Polyimide (cPI), and Cross-Linked Polybenzoxazole (cPBO).** In a 100 mL round flask were added 30 mL of DMAc (g), 5 (2.6 g, 5 mmol), and BTDA (1.61 g, 5 mmol). The mixture was stirred for 12 h at room temperature to obtain poly(BZaa). Then, the viscous poly(BZaa) solution was cast over a glass plate by a slicker, dried overnight at 80 °C, and then heated at 100 °C (1 h), 200 °C (1 h), and 300 °C (1 h) to obtain cPI. The cPI can be further treated at 400 °C for 1 h and then obtain cPBO.

## RESULTS AND DISCUSSION

### Preparation of *ortho*-Amine-Functional Benzoxazines.

The pathway adopted for obtaining amine-functional benzoxazines started from amine-protected phenols for preparation of benzoxazine monomers and then deprotected to liberate the amine. Tetrachlorophthalimide (TCP)-protected aminophenol (**1**) was synthesized and used for preparation of *ortho*-amine-monofunctional (**3**) and difunctional (**5**) benzoxazines at the first stage, as shown in Scheme 2. TCP-protected monofunctional benzoxazine (**2**) was synthesized from the Mannich condensation of **1**, paraformaldehyde, and aniline. Then primary amine-monofunctional benzoxazine monomer (**3**) can be achieved by deprotection of **2**. *o*-TCP-protected bifunctional benzoxazine (**4**) was prepared from **1**, paraformaldehyde, and DDM, followed by deprotection to give **5**. In this case for preparing difunctional monomer **4**, a considerable amount of gel formed, which was observed during the early stage of the synthesis, all disappeared overnight. A transparent solution was subsequently formed, leading to a high yield. On the contrary, in our previous work, a *p*-TCP-protected bifunctional benzoxazine showed a significant amount of gel formation, and the insoluble gel did not disappear even after a long reaction time was employed, resulting in a poor yield.<sup>15</sup> One possibility for the high yield of **4** is that the intramolecular 7-membered hydrogen bond between the phenolic OH group and one of the carbonyl group, albeit weak interaction, decreases the polarity of **1**, which improves the solubility of **1** in aprotic solvent. At the same time, the intramolecular hydrogen bond also accelerates the ionization of phenolic OH group during the initial stage for forming benzoxazine ring. The deprotection of TCP to amine was easily achieved by using chloroform solution of hydrazine monohydrate in a reasonable high yield.

The structures of TCP-protected benzoxazines were confirmed by  $^1\text{H}$  NMR and FTIR analyses. As shown in Figure 1, the characteristic resonances attributed to the benzoxazine structure, Ar– $\text{CH}_2$ –N–, and –O– $\text{CH}_2$ –N– for **2** and **4** are observed at 4.73 and 5.44 ppm and 4.66 and 5.37 ppm, respectively. Also, the  $^1\text{H}$  NMR spectra confirm the presence of methylene group (– $\text{CH}_2$ –) at 3.71 ppm for **4**.

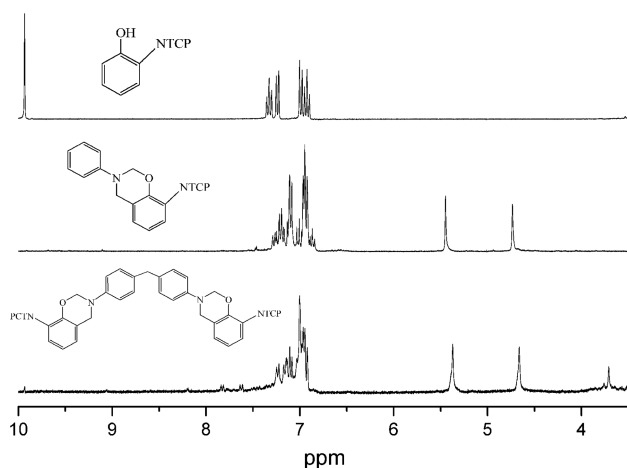


**Figure 1.**  $^1\text{H}$  NMR of TCP-protected phenol (1), TCP-protected monobenzoxazine (2), and TCP-protected bisbenzoxazine (4).

The structure of monoamine and diamine-functional benzoxazine monomers **3** and **5**, respectively, were also confirmed by  $^1\text{H}$  NMR and FTIR analyses. As shown in Figure 2, the characteristic resonances attributed to the benzoxazine

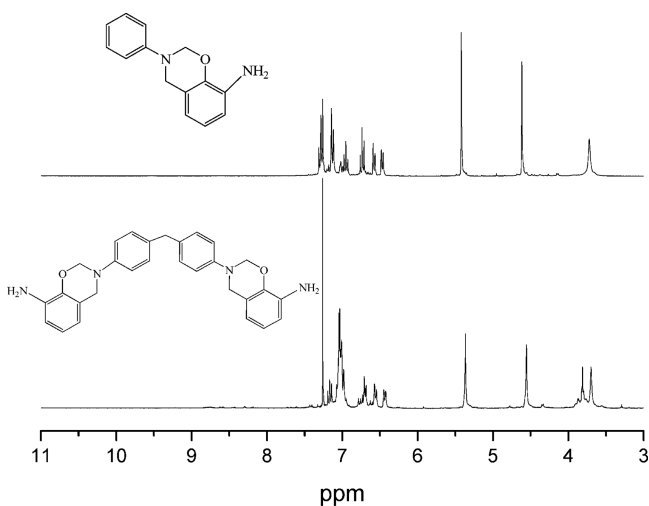


**Figure 2.**  $^1\text{H}$  NMR of amine-functional monobenzoxazine (3) and amine-functional bisbenzoxazine (5).

structure,  $\text{Ar}-\text{CH}_2-\text{N}-$ , and  $-\text{O}-\text{CH}_2-\text{N}-$  for **3** and **5** are observed at 4.62 and 5.42 ppm and 4.56 and 5.37 ppm, respectively. The resonance appeared due to the  $-\text{NH}_2$  protons at 3.72 ppm for monofunctional benzoxazine **3** and 3.69 ppm for bifunctional benzoxazines **5**. Also, the  $^1\text{H}$  NMR spectra confirm the presence of methylene group ( $-\text{CH}_2-$ ) at 3.81 ppm for **5**.

Figure 3 shows the FTIR spectra of benzoxazine **3** and **5**. The bands from the  $\text{C}-\text{O}-\text{C}$  antisymmetric stretching mode are at  $1222\text{ cm}^{-1}$  for the monofunctional and  $1230\text{ cm}^{-1}$  for the bifunctional benzoxazines. Besides, the characteristic out-of-plane absorption modes of benzene with an attached oxazine ring are observed at  $930\text{ cm}^{-1}$  for monofunctional benzoxazine and  $928\text{ cm}^{-1}$  in the case of difunctional benzoxazine.<sup>22,23</sup> The characteristic stretching bands of the primary amine appear at  $3483$ ,  $3373$ , and  $3320\text{ cm}^{-1}$  for the monofunctional benzoxazine and at  $3456$ ,  $3357$ , and  $3205\text{ cm}^{-1}$  for the bifunctional benzoxazine.

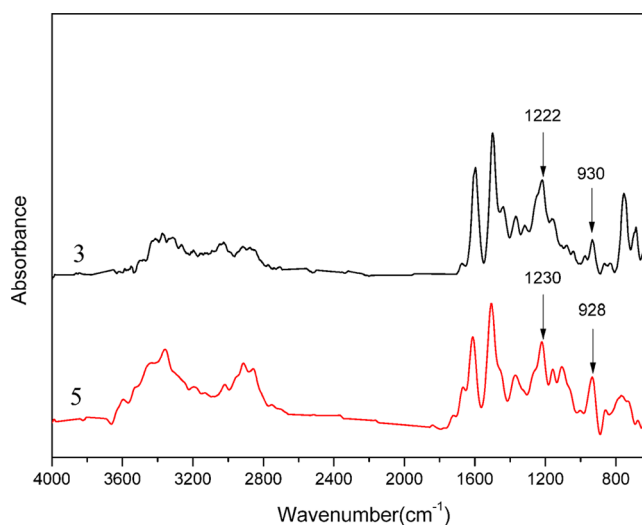
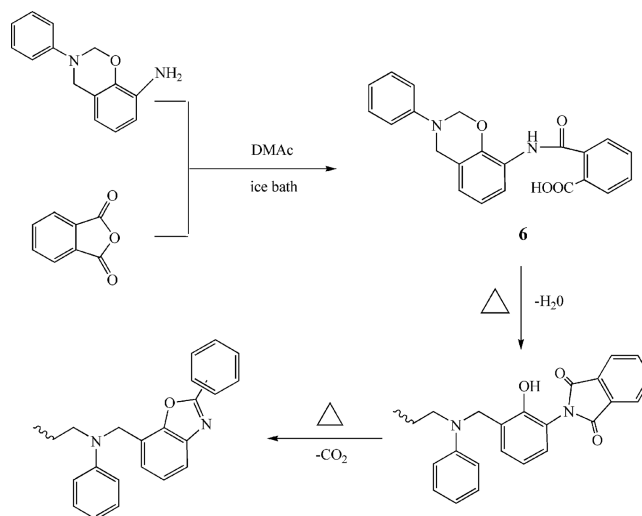


**Figure 3.** FTIR spectra of **3** and **5**.

**Preparation and the Polymerization, Thermal Imidization, and Thermal Cyclization Behavior of Benzoxazine Amic Acid Model Compound (6).** Model reaction between phthalic anhydride and **3** was performed to obtain benzoxazine amic acid compound **6** (Scheme 3). Figure 4

**Scheme 3.** Preparation and Thermal Treatment of **6**



shows the  $^1\text{H}$  NMR spectrum of **6**. The disappearance of the amine signal ( $3.72\text{ ppm}$ ) and the appearance of an amide signal ( $10.30\text{ ppm}$ ) support the reaction of amino and anhydride. However, a small peak at  $4.39\text{ ppm}$  was found in Figure 4. It is known that acid can catalyze the ring-opening reaction of benzoxazine; thus, the small peak is likely due to the methylene from the small amount of ring-opened structure. FT-IR was used to further confirm the structure of **6**. In Figure 5, a broad OH absorption of carboxylic acid absorption at around  $3412\text{ cm}^{-1}$ , a carbonyl absorption at  $1721\text{ cm}^{-1}$ , and the amide I mode at  $1681\text{ cm}^{-1}$  support the structure of amic acid. Complex and broad bands centered around  $3400\text{ cm}^{-1}$  are characteristic NH and OH bands that are strongly hydrogen bonded intramolecularly, further supporting the formation of amic acid.



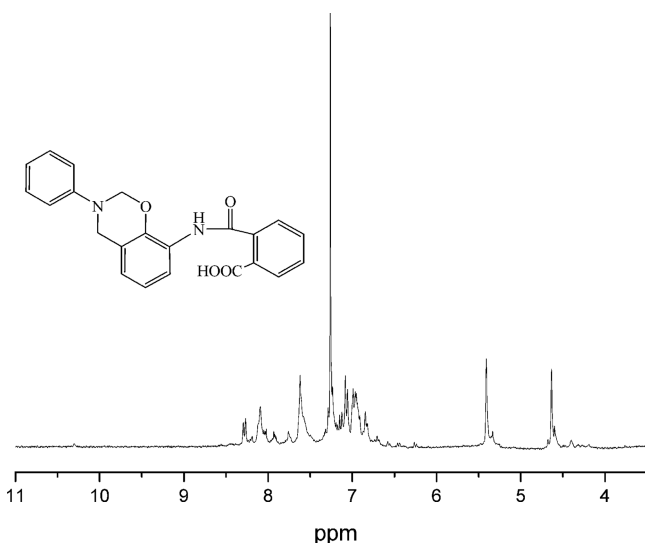


Figure 4.  $^1\text{H}$  NMR of benzoxazine amic acid (**6**).

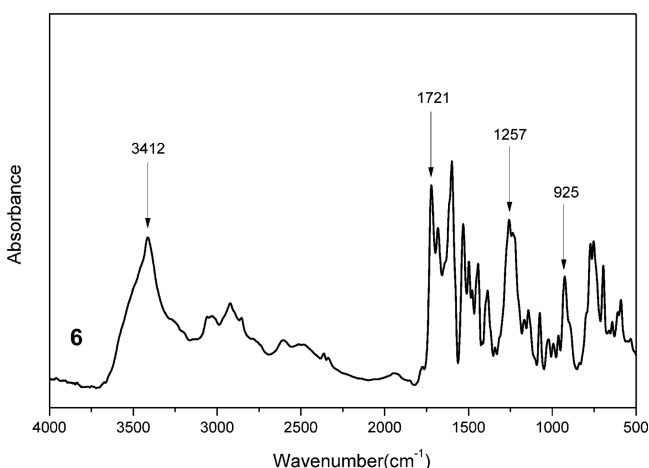


Figure 5. FTIR spectrum of **6**.

In order to qualitatively study the structural evolution of **6** during heating, FTIR analyses were carried out and the spectra are displayed in Figure 6. As shown in Figure 6, the characteristic absorption bands at  $1236\text{ cm}^{-1}$  (C–O–C

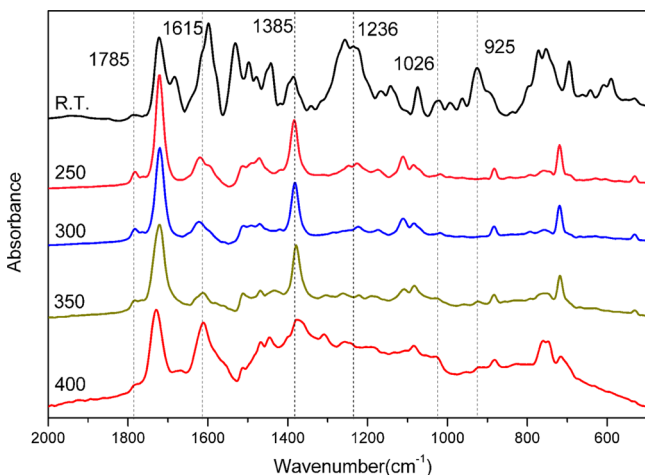


Figure 6. FTIR spectra of **6** after various thermal treatments.

asymmetric stretching mode) and  $925\text{ cm}^{-1}$  (the out-of-plane bending vibration of C–H) disappeared at  $250\text{ }^{\circ}\text{C}$ , corresponding to the ring-opening of benzoxazine. Meanwhile, new characteristic absorptions of imide at  $1785$  and  $1385$  are observed due to the imidization of amic acid. The characteristic peaks at  $1785\text{ cm}^{-1}$  are the typical peaks for imide, which is attributed to the imide C–C(=O)–C in-phase stretching.<sup>24</sup> The peak at  $1385\text{ cm}^{-1}$  is the axial C–N stretching.<sup>25</sup> However, these characteristic peaks for imide gradually decrease when heated from  $300$  to  $400\text{ }^{\circ}\text{C}$ , and meanwhile two peaks at  $1615\text{ cm}^{-1}$  (C=N stretching) and  $1026\text{ cm}^{-1}$  (–O–C stretching) gradually increase. This behavior is consistent with the benzoxazole ring formation after the benzoxazine ring-opening and further imidization.<sup>26,27</sup>

In order to further support the imidization and benzoxazole formation of **6**, the thermal stability of **6** has been studied by thermogravimetric analysis (TGA) as shown in Figure 7 after

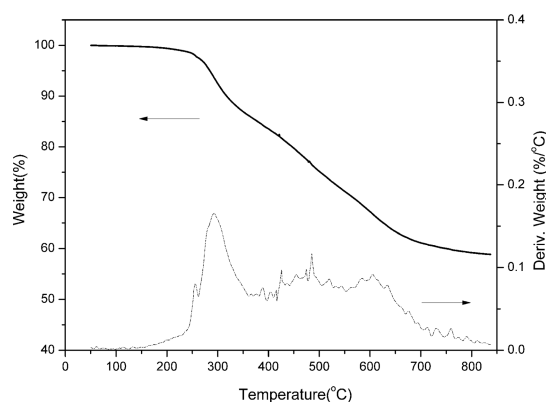


Figure 7. Thermogravimetric analysis of **6** after thermal polymerization at  $200\text{ }^{\circ}\text{C}$  for 1 h.

thermal treatment at  $200\text{ }^{\circ}\text{C}$ . It is well-established that the polymerization of benzoxazines occurs through oxazine ring-opening without producing any byproduct and the thermal degradation of polybenzoxazines starts over  $300\text{ }^{\circ}\text{C}$ .<sup>28</sup> However, **6** shows a weight reduction at very low temperature. As shown from the derivative weight loss curves, the maximum weight loss rate is around  $300\text{ }^{\circ}\text{C}$ , which is due to the imidization before  $300\text{ }^{\circ}\text{C}$  and the cyclization to form benzoxazole after  $300\text{ }^{\circ}\text{C}$ . Thus, both the results of FTIR and TGA are practically identical to those reported for polybenzoxazole synthesized through the traditional approach of the linear poly(*o*-hydroxyimide) method, indicating that thermal imidization and benzoxazole formation have been completed.

**Preparation of Poly(BZaa), cPI, and cPBO.** The preparation of poly(BZaa) was performed by reacting **5** and BTDA with a molar ratio of 1:1 (Scheme 4). The mixture was reacted at room temperature to form poly(BZaa), followed by a thermal treatment to imidize and cross-link benzoxazine to form cPI, and the further thermal treatment to form cPBO.

**DSC Thermograms of Benzoxazines.** It is well-known that the ring-opening polymerization reaction of 1,3-benzoxazine can be monitored by DSC with an exothermic peak around  $250\text{ }^{\circ}\text{C}$ .<sup>28</sup> Figure 8 shows the DSC thermograms of the TCP-protected benzoxazine monomers **2** and **4**. Monomer **2** exhibits an endotherm at  $194\text{ }^{\circ}\text{C}$  due to melting and a typical DSC benzoxazine exotherm maximum at  $222\text{ }^{\circ}\text{C}$ . However, the melting endotherm and polymerization exotherm maximum for

## Scheme 4. Preparation of Poly(BZaa), CPI, and CPBO

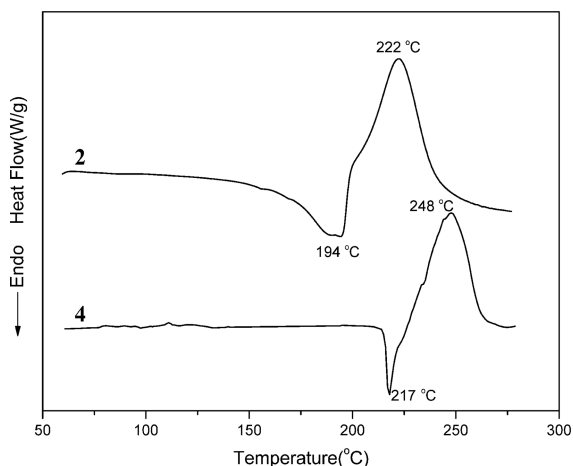
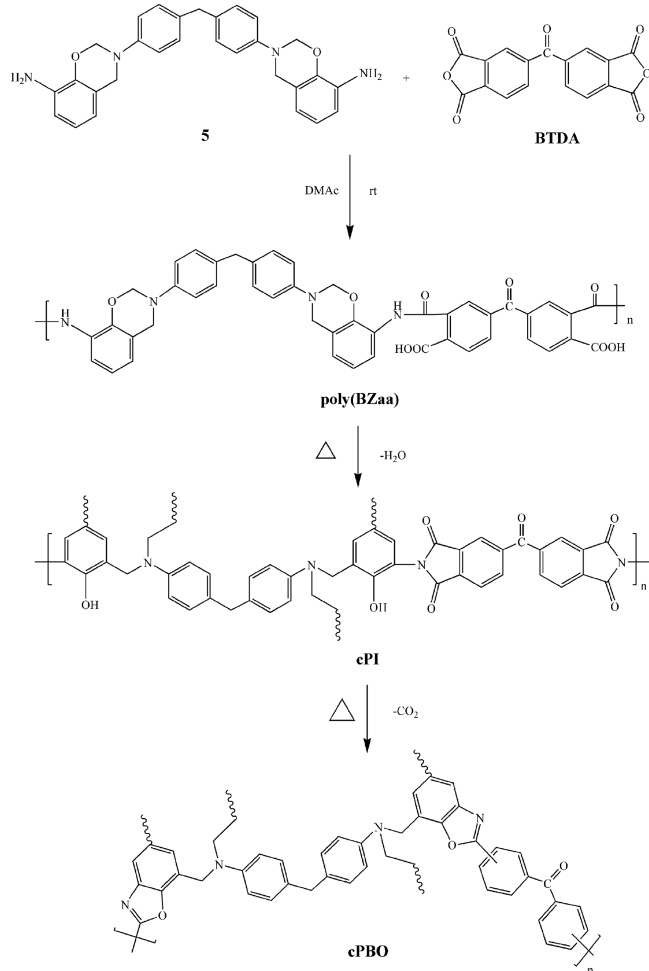


Figure 8. DSC thermograms of TCP-protected benzoxazine monomers 2 and 4.

difunctional monomer 4 are shifted to as high as 217 and 248 °C, respectively. Different from TCP-protected benzoxazine monomers, the primary amine-functional benzoxazine shows multiple thermal behaviors in the form of several exotherms as shown in Figure 9. Two exothermic peaks were observed with the maxima at 149, 183 °C and 151, 204 °C for monomers 3 and 5, respectively, which is in part due to the primary amine group catalyzing the ring-opening of benzoxazine.<sup>29,30</sup>

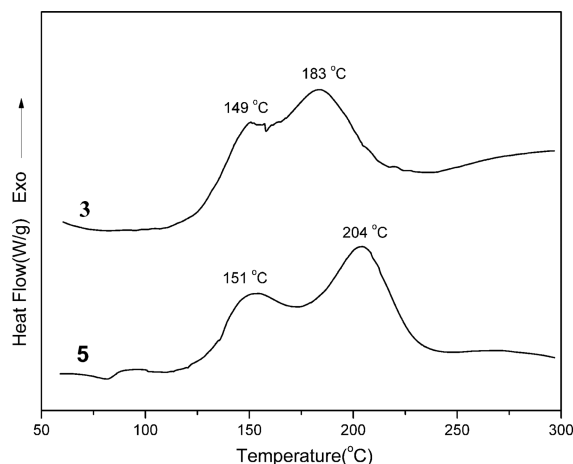


Figure 9. DSC thermograms of primary amine-functional benzoxazine monomers 3 and 5.

Figure 10 shows the DSC thermograms of benzoxazine amic acid model compound 6 and main-chain-type poly(BZaa). The

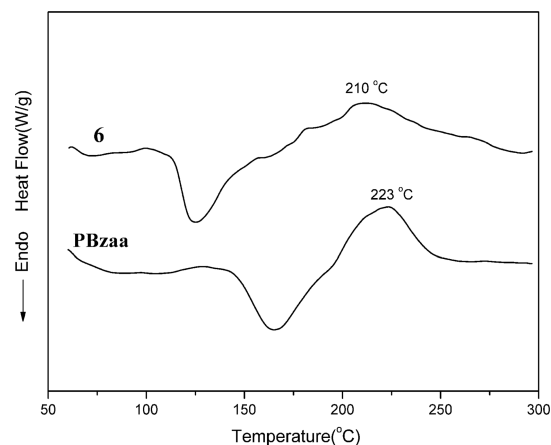
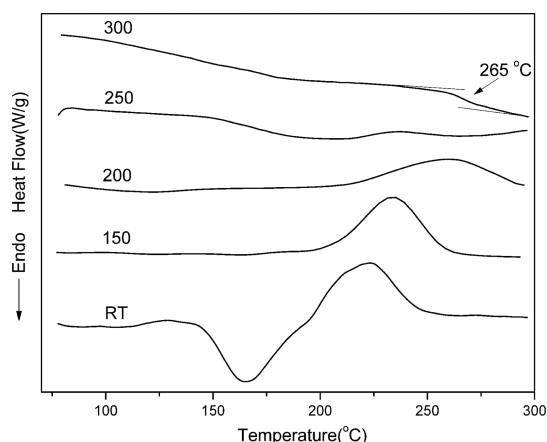


Figure 10. DSC thermograms of benzoxazine amic acid model compound 6 and main-chain-type poly(BZaa).

broad solvent-related endothermic peaks were observed for both 6 and poly(BZaa). To minimize oxazine ring-opening by the acid catalysis, we avoided removing the solvent completely, which requires heating the sample. An exothermic peak with maxima at 210 and 223 °C can be observed for 6 and poly(BZaa), respectively. The exothermic peaks show broader shape compared with traditional benzoxazines, which is due to the imidization taking place during the polymerization behavior. It is well-known that imidization is an endothermic behavior with the release of water, and thus, the observed apparent exothermic peak is the sum of exothermic and endothermic events. However, we could not calculate the enthalpy for the ring-opening since the solvent evaporation and imidization changed the weight of sample during the DSC measurement.

**DSC Analysis of Poly(BZaa) as a Function of Heat Treatment.** The thermally activated cross-linking behavior of the main-chain-type poly(benzoxazine amic acid) (PBZaa) by ring-opening was also studied by DSC. Figure 11 shows the DSC thermograms of poly(BZaa) after thermal treatment at 150, 200, 250, and 300 °C for 1 h at each temperature. It was found that the exothermic peak decreased after each treatment



**Figure 11.** DSC thermograms of poly(BZaa) after various thermal treatments.

temperature and practically disappeared at 250 °C, thereby showing the completion of the ring-opening polymerization reaction. After further thermal treatment at 300 °C, the product of poly(BZaa) showed a  $T_g$  as high as 265 °C.

**Thermal Properties of Cross-Linked cPI and cPBO.** The results of dynamic mechanical analysis (DMA) of the thermosets are as shown in Figure 12 for the storage modulus ( $E'$ ), loss modulus ( $E''$ ), and  $\tan \delta$ . In this work, the peak of  $\tan \delta$  is used to mark the glass transition temperature ( $T_g$ ). As shown in Figure 12 (top), the  $T_g$  determined as the peak

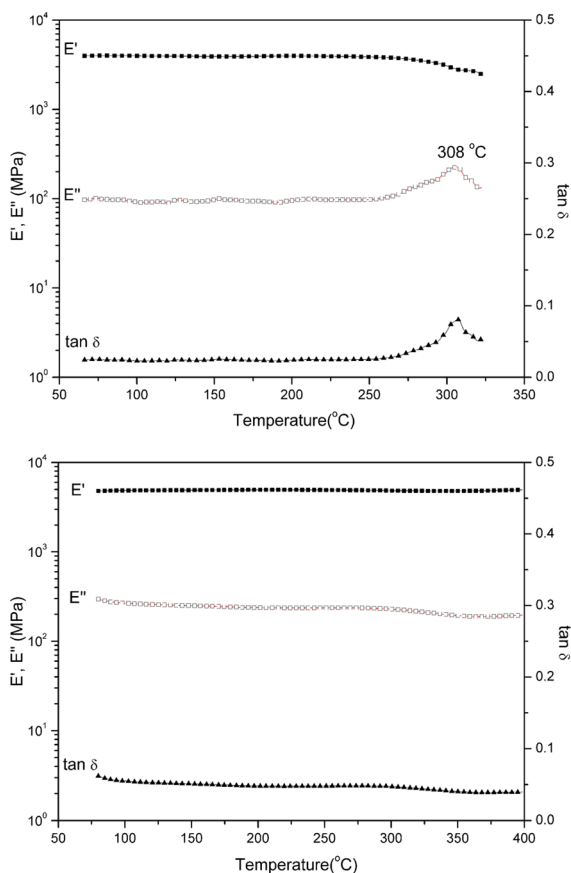


**Figure 12.** Dynamic mechanical spectra of cPI (top) and cPBO (bottom).

temperature of the  $E''$  curve is around 308 °C for cPI, which means even the value of  $T_g$  for cPI in this study is similar to that of polybenzoxazoles via thermal conversion from *ortho*-amide-functional benzoxazines in our previous study.<sup>14</sup> However, the cPBO shows no  $T_g$  before 400 °C as shown in Figure 12 (bottom), which means that this material can be applied at a very high temperature. We did not examine the behavior at higher temperatures to find the  $T_g$  because the degradation of polybenzoxazine segments takes place after 400 °C. Based on the TGA thermogram of cPBO shown in a later section, the degradation starts mostly around 500 °C. However, the scanning rate of the DMA (3 °C/min) is slower than the TGA experiment (10 °C/min). Considering this, we could not confidently examine the  $T_g$  above 400 °C.

Of particular interest is the remarkable constancy of the  $E'$  value of 5 GPa throughout the temperature range examined up to 400 °C. While there are many polymers that show relatively high  $T_g$ s, one seldom find materials with nearly constant  $E'$  throughout the temperature range examined. This is a particularly attractive property for an application with a wide temperature variation during the application in addition to a constant, elevated temperature.

The thermal stability of cPI and cPBO has been studied by thermogravimetric analysis (TGA), and the result is shown in Figure 13. In order to further confirm the imidization and

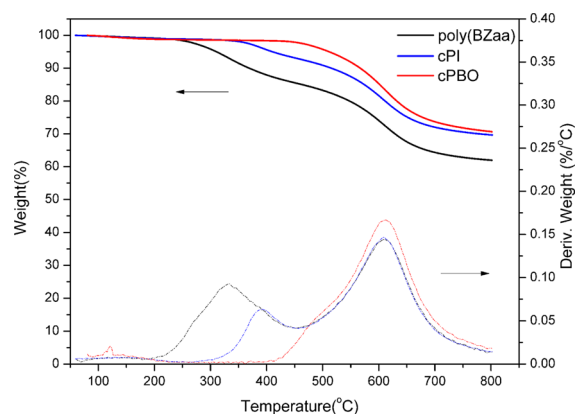


**Figure 13.** Thermogravimetric analysis of poly(BZaa) after thermal polymerization at 200 °C for 1 h, cPI, and cPBO.

benzoxazole formation of benzoxazine amic acid, we also studied the thermal stability of poly(BZaa) after the thermal treatment at 200 °C for 1 h. In comparison, this poly(BZaa) was further treated at 300 °C for 1 h, and its TGA thermogram is designed as cPI in the same figure. Additionally, the cPI was further treated at 400 °C for 1 h and designed as cPBO. The TGA thermograms of these cPI and cPBO are also shown in Figure 13. Poly(BZaa) shows a bimodal degradation profile in which the maximum weight-loss rate is at 330 °C, which corresponds to the typical imidization temperature. This lower temperature profile appears to be heavily overlapped multiple phenomena. cPI also shows a bimodal degradation profile in which the maximum weight-loss rate of the first step occurs at 400 °C, which indicates the thermal cyclization to give polybenzoxazole.

The thermal property data of cPI and cPBO are summarized in Table 1. The 5% weight loss temperatures ( $T_{d5}$ ) are as high as 410 and 511 °C for cPI and cPBO, respectively, as a consequence of the imide and oxazole formation. Besides, cPI

Table 1. Thermal Properties of CPI and CPBO

sample	$T_g$ (DSC) (°C)	$T_g$ (DMA) (°C)	$T_5$ (°C)	$T_{10}$ (°C)	$Y_c$ (wt %)
cPI	265	308	410	515	70
cPBO			511	567	71

and cPBO show very high char yield values of 70% and 71%, respectively. The data demonstrate the high thermal stability of cPI and the superhigh thermal stability of cPBO thermosets.

Figure 14 shows the Raman spectrum of the char derived from cPBO after the TGA measurement. As shown in Figure

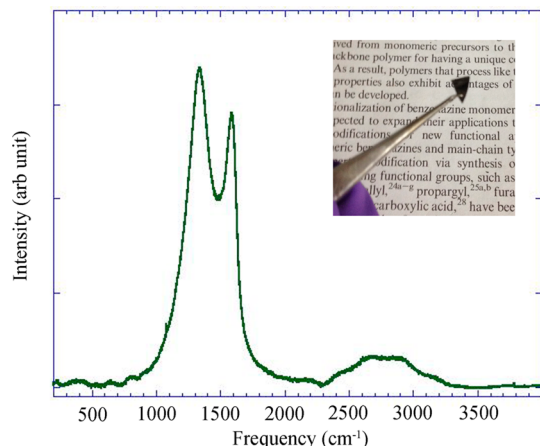


Figure 14. Raman spectra for the char of cPBO after TGA measurement. The inset is a photo of the char.

14, the peaks observed at 1585 and 1340  $\text{cm}^{-1}$  are attributed to the G (stretching mode of graphite) and D (breathing mode) bands, respectively. The Raman spectrum suggests that this char is consistent with the amorphous carbon rather than graphitic. Besides, this char can keep the shape with the reasonable mechanical properties after the thermal degradation at 800 °C.

## CONCLUSIONS

A new approach has been achieved to synthesize both cross-linked polyimide and cross-linked polybenzoxazole by incorporating benzoxazine and *o*-imide structure as a repeating unit in the main chain. Benzoxazine resin was used as the precursor for the eventual benzoxazole structure. This approach offers advantages for synthesizing highly thermally stable, cross-linked polybenzoxazole with easier processing conditions than the traditionally used methods. In aiming at better understanding the synthesis reaction, polymerization, imidization, and benzoxazole formation, a model compound was synthesized from the primary *ortho*-amine-functional benzoxazine with phthalic anhydride in dimethylacetamide as solvent. The polymers after thermal treatment showed excellent thermal stability appointing these materials to a good candidate for the high performance and even superhigh performance applications.

## AUTHOR INFORMATION

### Corresponding Author

\*E-mail: hxi3@cwru.edu (H.I.).

### Notes

The authors declare no competing financial interest.

## ACKNOWLEDGMENTS

K. Zhang gratefully acknowledges the partial financial support of Chinese Scholarship Council (CSC) Program.

## REFERENCES

- (1) Meador, M. A. *Annu. Rev. Mater. Sci.* **1998**, 28, 599–630.
- (2) Jaffe, M.; Haider, M. I.; Menczel, J.; Rafalko, J. *Polym. Eng. Sci.* **1992**, 32, 1236–1241.
- (3) Feng, D. D.; Wang, S. F.; Zhuang, Q. X.; Guo, P. Y.; Wu, P. P.; Han, Z. W. *J. Mol. Struct.* **2004**, 707, 169–177.
- (4) Fukumaru, T.; Fujigaya, T.; Nakashima, N. *Macromolecules* **2012**, 45, 4247–4253.
- (5) Fukumaru, T.; Saegusa, Y.; Fujigaya, F.; Nakashima, N. *Macromolecules* **2014**, 47, 2088–2095.
- (6) Ning, X.; Ishida, H. *J. Polym. Sci., Part A: Polym. Chem.* **1994**, 32, 1121–1129.
- (7) Ishida, H.; Rodriguez, Y. *Polymer* **1995**, 36, 3151–3158.
- (8) Endo, T.; Sudo, A. *J. Polym. Sci., Part A: Polym. Chem.* **2009**, 47, 2847–2858.
- (9) Zhang, K.; Zhuang, Q. X.; Zhou, Y. C.; Liu, X. Y.; Yang, G.; Han, Z. W. *J. Polym. Sci., Part A: Polym. Chem.* **2012**, 50, 5115–5123.
- (10) Yagci, Y.; Kiskan, B.; Ghosh, N. N. *J. Polym. Sci., Part A: Polym. Chem.* **2009**, 47, 5565–5576.
- (11) Tuzun, A.; Kiskan, B.; Alemdar, N.; Erciyes, A. T.; Yagci, Y. *J. Polym. Sci., Part A: Polym. Chem.* **2010**, 48, 4279–4284.
- (12) Zhang, K.; Zhuang, Q. X.; Liu, X. Y.; Yang, G.; Cai, R. L.; Han, Z. W. *Macromolecules* **2013**, 46, 2696–2704.
- (13) Liu, J.; Ishida, H. *Macromolecules* **2014**, 47, 5682–90.
- (14) Agag, T.; Liu, J.; Graf, R.; Spiess, H. W.; Ishida, H. *Macromolecules* **2012**, 45, 8991–8997.
- (15) Agag, T.; Arza, C. R.; Mauer, F. H. J.; Ishida, H. *Macromolecules* **2010**, 43, 2748–2758.
- (16) Agag, T.; Arza, C. R.; Mauer, F. H. J.; Ishida, H. *J. Polym. Sci., Part A: Polym. Chem.* **2011**, 49, 4335–4342.
- (17) Wang, M. W.; Lin, C. H.; Juang, T. Y. *Macromolecules* **2013**, 46, 8853–8863.
- (18) Tullios, G. L.; Powers, J. M.; Jeskey, S. J.; Mathias, L. J. *Macromolecules* **1999**, 11, 3598–3612.
- (19) Okabe, T.; Morikawa, A. *High Perform. Polym.* **2008**, 20, 53–66.
- (20) Park, H. B.; Jung, C. H.; Lee, Y. M.; Hill, A. J.; Pas, S. J.; Mudie, S. T.; Wagner, E. V.; Freeman, B. D.; Cookson, D. J. *Science* **2007**, 318, 254–258.
- (21) Wang, H.; Liu, S.; Chung, T. S.; Chen, H.; Jean, Y. C.; Pramoda, K. P. *Polymer* **2011**, 52, 5127–5138.
- (22) Agag, T.; Takeichi, T. *Macromolecules* **2003**, 36, 6010–6017.
- (23) Dunkers, J.; Ishida, H. *Spectrochim. Acta* **1995**, 51 A, 1061–1074.
- (24) Ishida, H.; Wellinghoff, S. T.; Baer, E.; Koenig, J. L. *Macromolecules* **1980**, 13, 826–834.
- (25) Low, B. T.; Xiao, Y.; Chung, T. S.; Liu, Y. *Macromolecules* **2008**, 41, 1297–1309.
- (26) Likhatchev, D.; Gutierrez-Wing, C.; Kardash, I.; Vera-Graziano, R. *J. Appl. Polym. Sci.* **1996**, 59, 725–735.
- (27) Bassignans, P.; Cogrossi, C.; Gandino, M. *Spectrochim. Acta* **1963**, 19, 1885–1897.
- (28) Ishida, H. In *Benzoxazine Resin Handbook*; Ishida, H., Agag, T., Eds.; Elsevier: Amsterdam, 2011; pp 3–81.
- (29) Takeichi, T.; Agag, T.; Zeidam, R. *J. Polym. Sci., Part A: Polym. Chem.* **2001**, 39, 2633–2641.
- (30) Alhwaige, A. A.; Agag, T.; Ishida, H.; Qutubuddin, S. *Biomacromolecules* **2013**, 14, 1806–1815.